Available online at www.sciencedirect.com
ScienceDirect
Electrochimica Acta 52 (2006) 1799–1804
ELECTROCHIMICA Acta
www.elsevier.com/locate/electacta

Nanostructures from directionally solidified NiAl–W eutectic alloys☆

Achim Walter Hassel*,[1], Andrew Jonathan Smith, Srdjan Milenkovic

Department of Interface Chemistry and Surface Engineering, Max-Planck-Institut für Eisenforschung GmbH, Max-Planck-Str. 1, 40237 Düsseldorf, Germany

Received 6 November 2005; received in revised form 19 December 2005; accepted 22 December 2005
Available online 6 June 2006

Abstract

A directionally solidified eutectic NiAl–W alloy was employed as a source for NiAl nanopore arrays, W-nanowire arrays and W-nanowires. The NiAl–W eutectic alloy containing 1.5 at.% W. A growth rate of 30 mm h^{-1} was used at a temperature gradient of 40 K cm^{-1} in a Bridgman-type directional solidification furnace. A combined stability diagram was derived from the Pourbaix diagrams of the three elements involved (Ni, Al, W). It allowed predicting proper conditions for the selective dissolution of either of the phases. Etching in a mixture of HCl:H_2O_2 released parallel aligned W-nanowires with a wire diameter of ~200 nm. The aspect ratio observed in these measurements was over 400. Selective electrodissolution of the W minor phase was possible in a neutral buffer at 0.5 V versus SHE. This procedure yielded regular nanopore arrays with pore diameters of ~200 nm. The pore density obtained was 8×10^{10} m^{-2}. The relative coverage of the wires or the corresponding pores in a cross section was 0.3%. For the material employed in this study a 12 μm^2 area corresponds to a single nanowire electrode. The potential of this material and the processing developed is discussed in terms of the production of nanofilters, nanoelectrode sensors, nanowire arrays and quantitative amounts of single crystalline tungsten nanowires.

Keywords: Eutectic alloy; Nanowire; Selective etching; Nanoelectrodes array

1. Introduction

Nanotechnology is of interest as devices can show unusual properties due to quantum confinement if the feature size falls below a certain value. Metallic nanowires show this behaviour only in the lower nm range (below 10 nm). But also mesoscale structures from 100 to 1000 nm can have favourable properties. Their link to electrochemistry can be either through an electrochemical step involved in the production method or through their potential use in electrochemistry.

Metallic nanowires can be produced by template-directed synthesis, involving either chemical or electrochemical deposition of the wires [1–4]. Gold nanowires for example have been fabricated on polycarbonate templates by pulsed-laser deposition combined with electrochemical plating [1], generating nanowire arrays with a high aspect ratio and a diameter between 100 and 600 nm after dissolution of the carbonate template. Arrays of Ni nanowires with a diameter of 30 nm have been electrodeposited in alumina membranes [2,3]. A large number of studies have been directed towards the use of anodic alumina oxide as a template. The procedures for preparing highly ordered alumina membranes were extensively described in the literature [5–8]. Both chemical and electrochemical deposition into the pores with a subsequent dissolution of the matrix and thus a release of the wires is possible [8,9]. These wires are usually polycrystalline, which can be a drawback for their application.

The advantages of ultramicroelectrodes or nanoelectrodes (nanodes) have been demonstrated for example for SECM [10,11] and stripping voltammetry [12].

When organised in an array, the resulting electrodes could combine the advantages of both the nanoelectrode and the signal intensity from a macroscopic electrode.

Directional solidification of a eutectic alloy is a method that can facilitate the nanostructuring of a material [13]. From here on this material will be referred to as *DS*–NiAl-X were *DS* indicates directionally processed material and NiAl-X indicates the quasibinary system consisting of the B2 NiAl phase and the minor phase X.

This method has several advantage. It produces arrays of single crystalline wires embedded in a single crystalline

☆ Presented in parts at the ISE meeting in Busan, Korea.
* Corresponding author. Fax: +49 211 6792 218.
E-mail address: hassel@elchem.de (A.W. Hassel).
[1] ISE active member.

0013-4686/$ – see front matter © 2006 Elsevier Ltd. All rights reserved.
doi:10.1016/j.electacta.2005.12.061

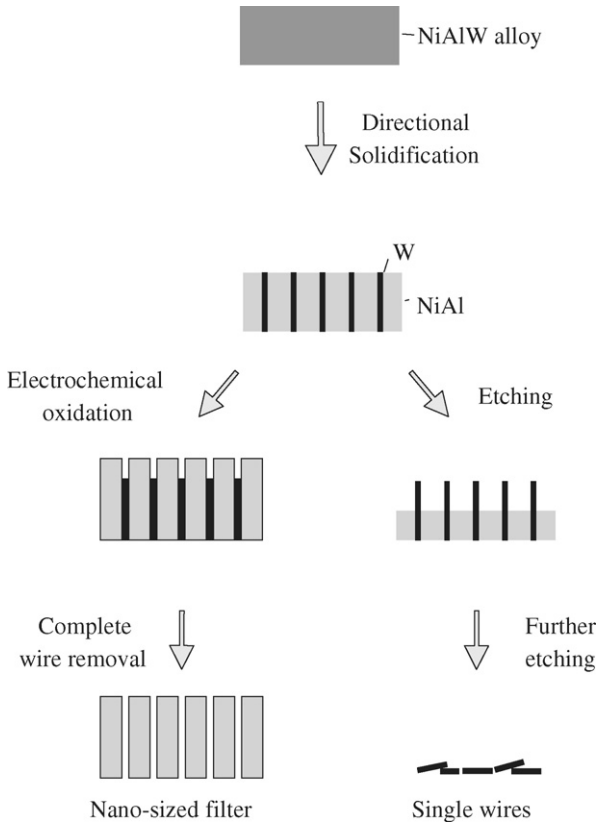

Fig. 1. Roadmap for the processing of *DS*–NiAl–W for the production of W-nanowire arrays, W-nanowires and NiAl nanopore arrays.

matrix. Wire diameter and spacing show a narrow distribution, and can be controlled by the processing parameters [13].

Digestion of the *DS*–NiAl–Re eutectic in an appropriate oxidising solution, and without application of an external voltage, resulted in the dissolution of both Ni and Al elements as Al (III) and Ni (II) ions, whereas Re stayed intact in that potential range [14,15]. Contrariwise the selective dissolution of the rhenium to perrhenate was achieved in a neutral buffer where the nickel aluminium major phase passivates [16]. The roadmap in Fig. 1 shows the processing of the corresponding *DS*–NiAl–W system, which is the topic of this paper.

2. Experimental

2.1. Preparation of the eutectic

Pre alloys were prepared from nickel (99.97 wt.%), electrolytic aluminium (99.99 wt.%) and tungsten (99.9 wt.%) by induction melting under an inert atmosphere. They were drop cast into a cylindrical copper mould and subsequently fitted into alumina crucibles. Directional solidification was performed in a Bridgman type crystal growing facility, consisting of the crucible support, cooling ring and heating element (tungsten net). The alumina crucible with the as-cast ingot was positioned in the furnace and heated up to ~1700 °C for initial melting. The upper part with the heating element was then slowly and uniformly shifted upwards to allow unidirectional heat extraction. This operation was controlled by a servomotor enabling a speed range between 1 and 200 mm h^{-1}. This solidification was conducted at a temperature of 1700 ± 10 °C, a thermal gradient of approximately 40 K cm^{-1} and a growth rate of 30 mm h^{-1}. The microstructure of the obtained unidirectionally solidified NiAl–W eutectic exhibited fully eutectic morphology consisting of a cell structure with a mean cell diameter of 500 μm and a length covering the entire length of the rod-like sample. A diameter of 200 nm was found for the tungsten wires and the mean inter fibre spacing was 3 μm. The fibre orientation was ⟨1 0 0⟩ referring to the rod axis of the directionally solidified sample.

2.2. Chemicals and electrodes

Digestion of the matrix was performed in a mixture of HCl (32%):H_2O_2 (30%):H_2O, 10:10:80. A self made Hg/Hg_2SO_4 reference electrode was used for the polarization experiments. The counter electrode was a strip of Pt foil with a surface area of 2 cm^2. Polarization was performed in acetate buffer with a pH of 6.0. All chemicals were of p.a. grade and purchased from Merck, Darmstadt.

2.3. Electronics

Electrochemical investigations of the samples were conducted with a PAR 283 potentiostat/galvanostat manufactured by EG & G.

Chemical analysis of the solutions was performed by inductively-coupled plasma optical emission spectrometry (ICP-OES).

Scanning electron microscopy was performed using a Leo 1550 VP apparatus (Leo Elektronenmikroskopie GmbH, Oberkochen, Germany) fitted with an INCA Energy Dispersive System (EDS) (Oxford Instruments, Oxford, UK).

3. Results and discussion

3.1. Construction of a combined stability diagram

In order to derive the optimum conditions for selectively etching the matrix as well as the optimum conditions for the selective formation of nanopores or nanochannels through removal of the wires the thermodynamic stability diagrams [17] of the elements in question were combined in Fig. 2.

The lines in the diagram depict the areas of relative predominance of the different species involved. For instance: at any given potential (above −1.7 V SHE) Al_2O_3 will corrode to Al^{3+} if the pH is reduced to values under 4.0 or it will corrode to AlO_2^- if the pH is increased to values greater than 9.0. The dashed lines indicate the thermodynamic range of the "electrochemical window"—the range in which electrochemical measurements can be performed without (equilibrium) evolution of H_2 (at potentials lower then the bottom dashed line) or O_2 (at potentials higher than the top dashed line). Further reactions which are essential for the intended procedures are given in the following two sections.

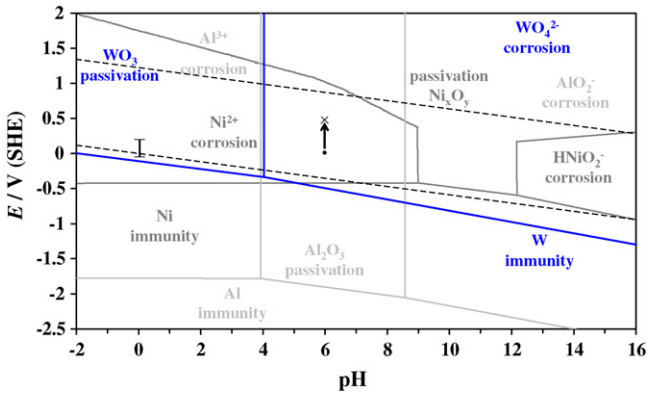

Fig. 2. Combined simplified pH-potential stability diagram derived from Pourbaix diagrams of the three elements Ni, Al, W. Matrix dissolution under etching conditions with simultaneous W passivation as well as selective electrodissolution of W with NiAl passivation are given in the diagrams.

3.2. Selective dissolution of the nickel–aluminium matrix

Based on the combined Ni–Al–W Pourbaix diagram reaction conditions were chosen under which both matrix elements nickel and aluminium should corrode whereas the tungsten would passivate. Acidic conditions were chosen (3.2% HCl) and the potential was chemically increased by an oxidising agent (3% H_2O_2). The *DS*–NiAl–W sample was immersed into an etching solution while monitoring the potential. As shown in Fig. 3 the potential oscillates between 0.150 and −0.025 V SHE while etching the matrix. The pH of this highly acidic solution was slightly below 0. The results of Fig. 3 are marked by a vertical bar in Fig. 2. As intended, this region lays well within the corrosion range of both nickel and aluminium. The horizontal line at approx. −0.5 V SHE marks the transition

$$\mathrm{Ni} \rightarrow \mathrm{Ni^{2+}} + 2\mathrm{e^-} \quad (1)$$

which lays significantly higher than the corresponding and thus parallel line for the less noble aluminium

$$\mathrm{Al} \rightarrow \mathrm{Al^{3+}} + 3\mathrm{e^-} \quad (2)$$

the vertical line at pH 4.0 marks the dissolution of the aluminiumoxide

$$\mathrm{Al_2O_3} + 6\mathrm{H^+} \rightarrow 2\mathrm{Al^{3+}} + 3\mathrm{H_2O}. \quad (3)$$

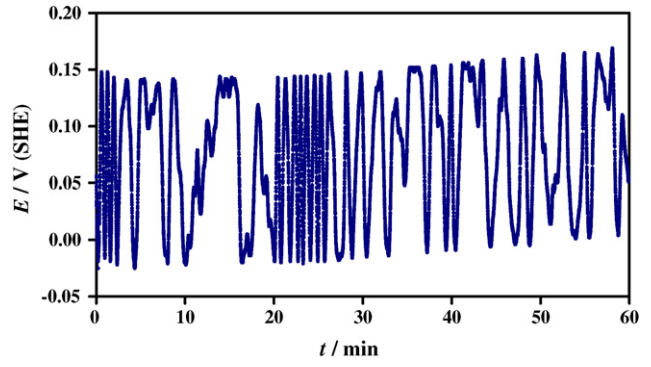

Fig. 3. Potential transient of matrix dissolution of *DS*–NiAl–W during 1 h in a mixture of 3.2% HCl and 3% H_2O_2.

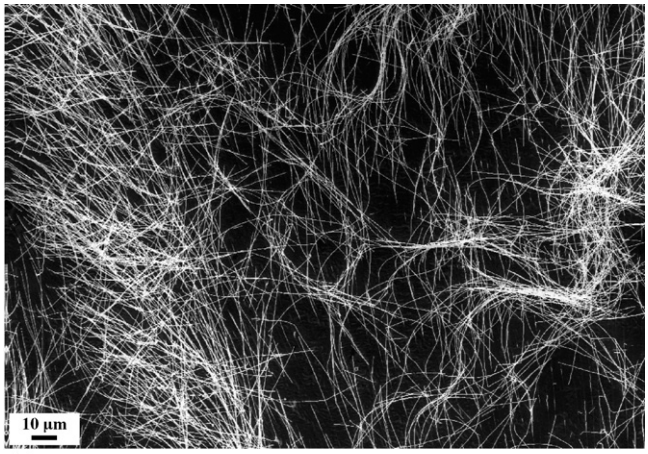

Fig. 4. (a) Long tungsten fibres observed on *DS*–NiAl–W after digestion for 1 h in a mixture of 3.2% HCl and 3% H_2O_2. (b) Side view of a tungsten nanowire array after digestion of NiAl matrix in 3.2% HCl and 3% H_2O_2 for 1 h.

For very anodic potentials nickel can passivate even in acidic solutions but these potentials, which would allow strong oxygen evolution are not reached by far in this solution. The combined Pourbaix diagram also displays that tungsten should exist as WO_3 under these conditions, preventing the dissolution of tungsten. A slightly more negative potential under which metallic tungsten is immune might work as well. However, a significant hydrogen evolution must be expected. Even under the chosen conditions bubbles formed on the surface and broke away continuously. These variations in the active wetted surface area are probably responsible for the fluctuations of the measured potential. A higher potential on the other hand would favor the WO_3 formation resulting in a larger oxide thickness.

Fig. 4a shows a top view of the *DS*–NiAl–W sample after 1 h of etching. It shows that a large number of nanowires with a length of several 100 μm are released from the matrix. Fig. 4b is a side view of the same sample. It clearly shows that these fibres are standing upright and parallel. Some broken wires are caught in this array. Fig. 5 shows an example of the extreme aspect ratio of these wires. The wire has a length of 87 μm and diameter of 200 nm from which an aspect ratio of more than 400

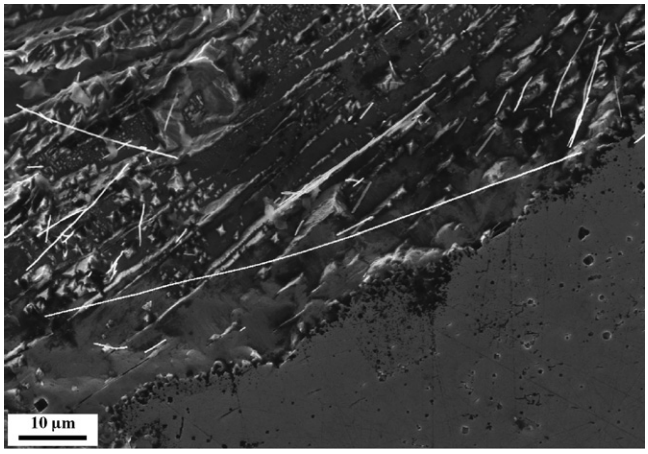

Fig. 5. Separated W wire resulting from the etching *DS*–NiAl–W.

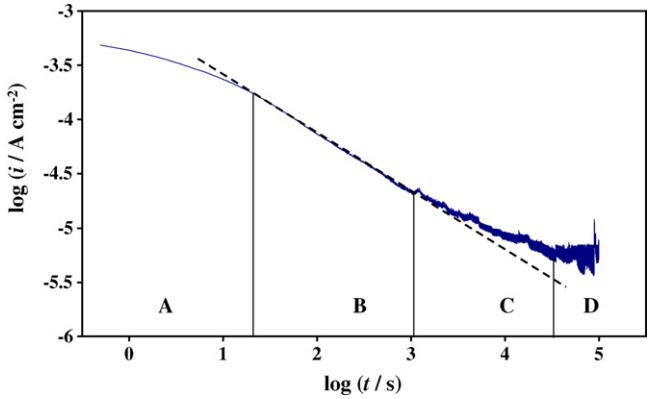

Fig. 6. Current transient of the electrodissolution of *DS*–NiAl–W eutectic alloy after selective electrodissolution of the W-minor phase in acetate buffer (pH 6.0) at 0.5 V (SHE) for 30 h.

is calculated. It is also important to keep in mind that these wires are single crystals.

Chemical analysis of the etching solution revealed concentrations of $c_{Al} = 178\,mg\,L^{-1}$, $c_{Ni} = 397\,mg\,L^{-1}$ and $c_W = 2.09\,mg\,L^{-1}$. Taking into account the atomic weights of the elements $M_{Al} = 26.98\,g\,mol^{-1}$, $M_{Ni} = 58.68\,g\,mol^{-1}$ and $M_W = 183.84\,g\,mol^{-1}$, contents of 49.28% (Al), 50.63% (Ni) and 0.07% are determined. To which extent the deviations from 50% for the two matrix elements are of relevance shall be evaluated in a later study. The small tungsten content in the etching solution may have two origins. It can either be the result of a very minor attack of the tungsten wires in the etching solution or it represents the tungsten that remained dissolved in the matrix during directional solidification. When etching the matrix the tip of a wire is released first and is in contact with the etching solution from then on. This would decrease the wire diameter as a function of exposure time. Since no such effect was observed in the SEM images, it is more likely that the W found in the solution results from the matrix.

3.3. Selective dissolution of the tungsten wires

The selective dissolution of the wires and thus the fabrication of nanopores were achieved by electrochemical processing of the material. The sample was immersed in acetate buffer with a pH of 6.0. After leaving the sample at open circuit potential (0.035 V SHE) for 10 min the potential was stepped to 0.5 V SHE and held for 30 h. The given pH provides optimum conditions for the passivation of Al

$$Al + 3H_2O \rightarrow Al_2O_3 + 6H^+ + 6e^- \quad (4)$$

whereas nickel, the second matrix element, would still corrode according to Eq. (1). Aluminium is a valve metal that can form very thick oxide layers. Under these conditions one would expect a dealloying that causes an enrichment of the aluminium on the surface which finally results in an aluminiumoxide film on top of the equiatomic NiAl alloy.

At the same time tungsten and tungsten oxide are dissolved according to

$$W + 4H_2O \rightarrow WO_4^{2-} + 8H^+ + 6e^- \quad (5)$$

and

$$WO_3 + H_2O \rightarrow WO_4^{2-} + 2H^+ \quad (6)$$

respectively.

Fig. 6 shows the current transient recorded during polarization. The potential jump causes simultaneous dissolution of nickel and tungsten according to Eqs. (1) and (5) in parallel to the passivation of aluminium (Eq. (4)). This is indicated as region A in Fig. 6. Aluminium oxide is known to grow according to the highfield model. This implies a −1 slope in a double logarithmic current over time plot. Such a slope is not observed since all three processes occur simultaneously and the time resolution is insufficient to see the very early stages, which are probably dominated by the passivation current. A direct comparison to a high resolution current transient of pure aluminium in an acetate buffer from the literature gives important information [18]. It shows that Debye charging of the oxide, dielectric relaxation of the oxide, charge carrier emission from the interfaces and initial highfield oxide growth take place already during the first second after stepping the potential. As a result of this self inhibiting process the current density is in the range of $1\,mA\,cm^{-2}$ and must be expected to further decrease with a −1 slope. It thus falls below the current observed for the *DS*–NiAl–W alloy in section B. This means that the alloy is already significantly passivated at the very beginning of the transient shown in Fig. 6. In region B of the transient the slope of the curve is almost exactly −0.5 indicating a diffusion controlled process. It is most likely that W is initially dissolved according to Eq. (5). This will create pores and a significant acidification in these pores, thus a shift in the equilibrium of Eq. (6) to the left side. For anodic potentials the Pourbaix diagram in Fig. 2 shows a vertical equilibrium line for Eq. (6) at pH = 4. The diffusion of protons into the bulk solution is linked to an increase of the pH within the pore. This shifts the equilibrium in Eq. (6) towards the soluble WO_4^{2-}. With increasing pore depth the diffusion length increases as well. This leads to a further decreasing current. After 1000 s the slope becomes

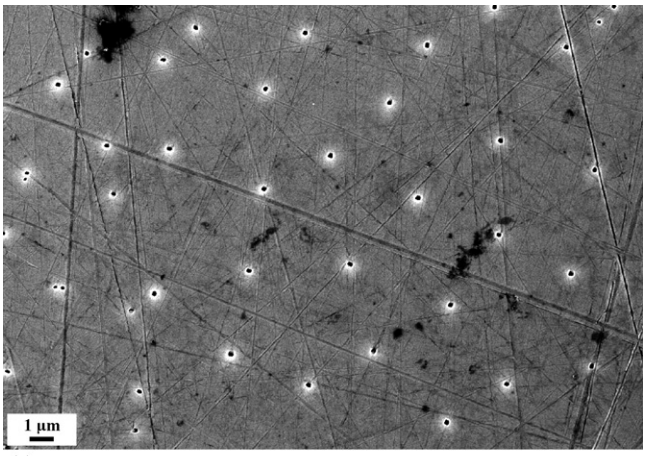

(a)

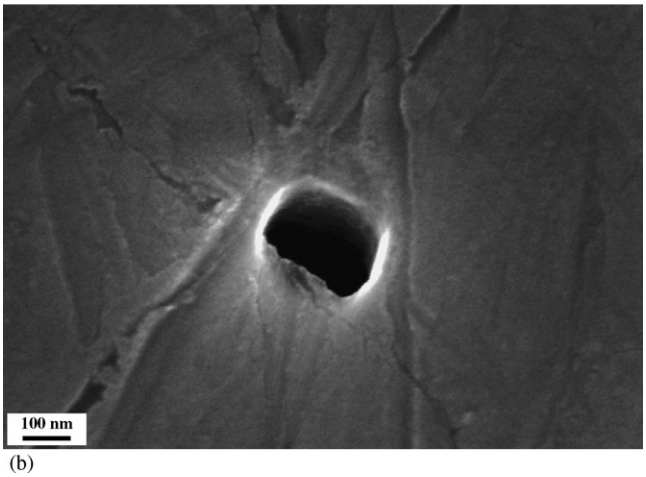

(b)

Fig. 7. (a) Nanopore array in a *DS*–NiAl–W eutectic alloy after selective electrodissolution of the W-minor phase in acetate buffer (pH 6.0) at 0.5 V (SHE) for 30 h. (b) Close view of a single nanopore in a *DS*–NiAl–W eutectic alloy after selective electrodissolution of the W-minor phase in acetate buffer (pH 6.0) at 0.5 V (SHE) for 30 h.

flatter and flatter in region C indicating that the current density of the stationary aluminiumoxide corrosion becomes more and more predominant. Finally in region D the current becomes constant—a phenomenon well known from pure aluminium.

Fig. 7a shows a SEM image of the *DS*–NiAl–W sample after this treatment. Pores are formed in the channels of the embedded tungsten wires. The pores are evenly distributed across the surface. The surface shown has a size of 511 μm^2. This allows computing a wire density of $8 \times 10^{10}\ m^{-2}$. Small scratches on the matrix resulting from the grinding are still visible demonstrating that the matrix does not dissolve.

A closer view into one of these pores is shown in Fig. 7b. The cross section shows that the hole is slightly elongated in one direction; the longer pore diameter is 245 nm and the shorter 170 nm. The two longer walls appear parallel; a strong hint on the faceted nature of the wires matrix interface.

A surface ratio of 0.3% W is calculated from these results. In average an area of 12 μm^2 can be attributed to each pore. All these values are important geometrical factors for the application of these electrodes as sensors in electroanalytical chemistry.

3.4. Strategic relevance of electrochemical processing of directionally solidified eutectics

A number of aspects have to be taken into account when electrochemical processing of directionally solidified material is considered for the preparation of nano or microstructured devices. If nanopore arrays shall be generated with or without redeposition of a metal into the pores, the nature of the minor alloying phase plays only a minor role. If on the other hand rods, wires or wire arrays of a certain metal shall be produced the major phase is of lesser importance. In both cases a significantly different chemistry or electrochemistry is required to allow selective dissolution. The phase diagram of the eutectic would ideally consist of pure phases rather than involving any intermetallic phase. It is desirable to have an asymmetric composition so that wires (guest phase) form in a matrix (host phase) and that the solubility of the pure phases in each other is as low as possible.

Governing the geometrical parameters namely wire diameter or pore diameter, respectively and inter fiber or inter pore spacing is straightforward. They can be controlled by the growth rate and the temperature gradient during directional solidification [19]. Higher growth rates yield both, smaller nanowire diameters and smaller interwire spacings.

It does not make much sense to compare directional solidification to methods that grow semiconductor wires from the gas phase. The method introduced here should rather be compared to methods that produce metallic nanowires in particular by chemical or electrochemical growth. Usually material with an array of nanochannels is employed. These materials can be produced by ion track etching into e.g. polymers, by hole (h^+) assisted photoetching of Si or by the fabrication of porous anodic aluminium oxide (AAO). The last method is by far the most important one. It is well established, can be handled at room temperature or at slightly elevated temperatures to produce metals or semiconductors or even alloys. Its production always requires a soluble precursor species, which is on the other hand responsible for some of the contaminations. The chemistry must be compatible with that of the solvent, e.g. the metal should not decompose or convert to its oxide. The method usually generates polycrystalline wires embedded in an isolating matrix. Processing of directionally solidified materials on the other hand is a self organizing process that does not require a template, even though the use of a template might be beneficial to increase the degree of order. The wires that form are single crystalline all having the same crystallographic orientation, even with the same azimuthal angle. This feature is of major importance for some applications, e.g. as field emitters. The composition of the wires is essentially that of the phase itself, presuming that sufficiently pure metals are employed for making the prealloy. Macroscopic cutting of the *DS*-material allows choosing the orientation in the sample and thus the application. Horizontal cuts allow the production of nanowire arrays while vertical cuts will produce nanowires aligned parallel to the surface. This cutting is relatively simple for the all metallic samples while it must be expected to be much more difficult for a system in which metal wires are embedded in ceramic matrix.

4. Conclusions

Directional solidification of a quasibinary NiAl–W eutectic alloy produced unidirectional nanostructured material. A strategy for selective removal of either of the two phases has been derived from a combined Pourbaix diagram of the three elements. A slightly oxidising acid dissolved the matrix and released an array of long and uniform tungsten wires. The high aspect ratio of these wires was demonstrated to be at least 435. Electrodissolution of the W to soluble WO_4^{2-} with a simultaneous passivation of the NiAl matrix yielded nanopore arrays with slightly elongated pores having a diameter of 170 nm in one direction and 245 nm in the other.

Electrodeposition of nobel metals such as gold into the pores as it was already demonstrated for the *DS*–NiAl–Re system is a promising route for the preparation of sensors [20]. The advantages of the *DS*–NiAl–W system over the *DS*–NiAl–Re system are the smaller wire diameters for identical solidification parameters and the smaller refractory metal content that increases the pore diameter to interspacing ratio. Dissolution of W through the entire sample thickness would yield a metallic nanofilter, a system with a number of advantages over ceramic filters.

Production of tungsten wires and even tungsten wire arrays becomes possible with the method shown here. The wire length can easily be controlled by the etching duration. Harvesting a decent amount of nanowires requires just the corresponding amount of alloy and a modification of the etching time. Last but not least it should be emphasized that quite a number of possible applications can be envisioned for single crystalline tungsten nanowires, which can hardly all be listed here.

Acknowledgement

The financial support of the Deutsche Forschungs Gemeinschaft through the project Production of Nanowire Arrays through Directional Solidification and their Application within the DFG Priority Program 1165 Nanowires and Nanotubes-from Controlled Synthesis to Function is gratefully acknowledged.

References

[1] W. Kautek, S. Reetz, S. Pentzien, Electrochim. Acta 40 (1995) 1461.
[2] K.R. Pirota, D. Navas, M. Hernández-Vélez, K. Nielsch, M. Vázquez, J. Alloys Compd. 369 (2004) 18.
[3] S.W. Lin, S.C. Chang, R.S. Liu, S.F. Hu, N.T. Jan, J. Magn. Magn. Mater. 282 (2004) 28.
[4] M. Wilms, J. Conrad, K. Vasilev, M. Kreiter, G. Wegner, Appl. Surf. Sci. 238 (2004) 490.
[5] H. Masuda, K. Fukuda, Science 268 (1995) 1466.
[6] H. Masuda, H. Yamada, M. Satoh, H. Asoh, M. Nakao, T. Tamamura, Appl. Phys. Lett. 71 (1997) 2770.
[7] H. Masuda, H. Asoh, M. Watanabe, K. Nishio, M. Nakao, T. Tamamura, Adv. Mater. 13 (2001) 189.
[8] N. Tao, J. Chem. Educ. 82 (2005) 720.
[9] Y. Piao, H. Lim, J.Y. Chang, W.-Y. Lee, H. Kim, Electrochim. Acta 50 (2005) 2997.
[10] V. Radtke, J. Heinze, Z. Phys. Chem 218 (2004) 103.
[11] K. Borgwarth, D. Ebling, J. Heinze, Electrochim. Acta 40 (1995) 1455.
[12] A.J. Bard, J. Allen, M. Stratmann, P.R. Unwin, R. Patrick, Encyclopedia of Electrochemistry Volume 3: Instrumentation and Electroanalytical Chemistry, Wiley-VCH, Weinheim, 2003, Chapter 2.3 Stripping Analysis by Joseph Wang ISBN 3-527-30395-2 p. 125.
[13] W. Kurz, P.R. Sahm, Gericht erstarrte Eutektische Wekstoffe, Springer, Berlin, 1975.
[14] R. Rablbauer, G. Frommeyer, F. Stein, Mater. Sci. Eng. A 343 (2003) 301.
[15] A.W. Hassel, B. Bello Rodriguez, S. Milenkovic, A. Schneider, Electrochim. Acta 50 (2005) 3033.
[16] A.W. Hassel, B. Bello Rodriguez, S. Milenkovic, A. Schneider, Electrochim. Acta 51 (2005) 795.
[17] M. Pourbaix, Atlas of Electrochemical Equilibria in Aqueous Solutions, National Association of Corrosion Engineers, Houston, 1974.
[18] M.M. Lohrengel, Mater. Sci. Eng. R11 (1993) 243.
[19] S. Milenkovic, A.W. Hassel, A. Schneider, Nano Lett. 6 (2006) 794.
[20] B. Bello Rodriguez, A. Schneider, A.W. Hassel, J. Electrochem. Soc. 153 (2006) C33.